Rosmarinic acid downregulates the oxLDL-induced interaction between monocytes and endothelial cells, in addition to monocyte diapedesis, under high glucose conditions

JEAN BAPTISTE NYANDWI[1-3*], YOUNG SHIN KO[1,2*], HANA JIN[1], SEUNG PIL YUN[1,2], SANG WON PARK[1,2], KEE RYEON KANG[4] and HYE JUNG KIM[1,2]

[1]Department of Pharmacology, College of Medicine, Institute of Health Sciences,
[2]Department of Convergence Medical Science (BK21 Plus), Gyeongsang National University, Jinju,
Gyeongsangnam-do 52727, Republic of Korea; [3]Department of Pharmacy, School of Medicine and Pharmacy,
College of Medicine and Health Sciences, University of Rwanda, Kigali 4285, Republic of Rwanda;
[4]Department of Biochemistry, College of Medicine, Institute of Health Sciences,
Gyeongsang National University, Jinju, Gyeongsangnam-do 52727, Republic of Korea

Abstract. Endothelial dysfunction during diabetes has been previously reported to be at least in part attributed to increased oxidized low-density lipoprotein (oxLDL) levels mediated by high glucose (HG) levels. Endothelial inflammation increases the adhesiveness of monocytes to the endothelium in addition to increasing vascular permeability, promoting diabetic atherogenesis. In a previous study, it was reported that oxLDL treatment induced nucleotide-binding domain and leucine-rich repeat containing family, pyrin domain-containing 3 inflammasome activation in endothelial cells (ECs) under HG conditions, in a manner that could be effectively reversed by rosmarinic acid. However, it remains unclear whether oxLDL-mediated inflammasome activation can regulate the interaction between monocytes and ECs. The effects of oxLDL-mediated inflammasome activation on endothelial permeability under HG conditions, in addition to the effects of rosmarinic acid on these oxLDL-mediated processes, also remain poorly understood. Therefore, the present study aimed to elucidate the mechanisms involved in oxLDL-induced endothelial permeability and monocyte diapedesis under HG conditions, in addition to the potential effects of rosmarinic acid. ECs were treated with oxLDL under HG conditions in the presence or absence of ROS scavengers mitoTEMPO and NAC, p38 inhibitor SB203580, FOXO1 inhibitor AS1842856 or transfected with the TXNIP siRNA, before protein expression levels of intercellular adhesion molecule 1 (ICAM-1), vascular cell adhesion molecule-1 (VCAM-1), phosphorylated vascular endothelial-cadherin (VE-cadhedrin), VE-cadherin and zonula occludens-1 (ZO-1) were measured by western blotting. In addition, adhesion assay and Transwell assays were performed. oxLDL was found to significantly increase the expression of ICAM-1 and VCAM-1 in ECs under HG conditions whilst also enhancing the adhesion of monocytes to ECs. This was found to be dependent on the reactive oxygen species (ROS)/p38 MAPK/forkhead box O1 (FOXO1)/thioredoxin interacting protein (TXNIP) signaling pathway. In addition, oxLDL-stimulated ECs under HG conditions exhibited increased phosphorylated VE-cadherin protein levels and decreased ZO-1 protein expression levels compared with those in untreated ECs, suggesting increased endothelial permeability. Furthermore, monocyte transmigration through the endothelial monolayer was significantly increased by oxLDL treatment under HG conditions. These oxLDL-mediated effects under HG conditions were also demonstrated to be dependent on this ROS/p38 MAPK/FOXO1/TXNIP signaling pathway. Subsequently, rosmarinic acid treatment significantly reversed oxLDL-induced overexpression of adhesion molecules and monocyte-EC adhesion, oxLDL-induced endothelial junction hyperpermeability and monocyte transmigration through the endothelial monolayer under HG conditions, in a

Correspondence to: Professor Hye Jung Kim, Department of Pharmacology, College of Medicine, Institute of Health Sciences, Gyeongsang National University, 816 Jinju-daero 15 Bungil, Jinju, Gyeongsangnam-do 52727, Republic of Korea
E-mail: hyejungkim@gnu.ac.kr

*Contributed equally

dose-dependent manner. These results suggest that rosmarinic acid can exert a protective effect against oxLDL-mediated endothelial dysfunction under HG conditions by reducing the interaction between monocytes and ECs in addition to preventing monocyte diapedesis.

Introduction

Endothelial cells (ECs) form a semi-permeable monolayer that separates the bloodstream from underlying tissues and regulate the infiltration of blood cells and proteins through the vessel wall (1,2). A number of studies have previously suggested that vascular endothelial dysfunction caused by increased junctional permeability is a key event in the development and progression of atherosclerosis and atherosclerotic cardiovascular diseases (3,4). Chronic metabolic disorders, such as hyperglycemia and dyslipidemia, promote endothelial dysfunction and eventually leakage, resulting in increased monocyte diapedesis (5-7). Endothelial dysfunction during diabetes is closely associated with increased oxidized low-density lipoprotein (oxLDL) levels mediated by high glucose (HG) conditions (8). HG and oxLDL induce oxidative stress by increasing the production of reactive oxygen species (ROS) (9), which drive inflammatory processes to mediate monocyte activation and recruitment to the inflamed endothelium (10). Subsequently, endothelial inflammation enhances the expression of intercellular adhesion molecule-1 (ICAM-1) and vascular cell adhesion molecule-1 (VCAM-1) on ECs to potentiate monocyte adhesion prior to diapedesis into the sub-endothelial space, which precedes atherosclerotic plaque development (11).

Endothelial permeability is regulated by the close cooperation between inter-endothelial cell adherens and tight junctions, which form an endothelial barrier to control the paracellular passage of blood constituents into the subendothelial space (2,12-16). Endothelial integrity is maintained by the highly coordinated opening and closing of endothelial adherens and tight junctions (17). Vascular endothelial (VE)-cadherin, a major constituent of adherens junctions, interacts with the tight junction molecule zonula occludens-1 (ZO-1) to link together adjacent ECs to regulate diapedesis (2,13). There is evidence that vascular permeability and leukocyte invasion are promoted by the phosphorylation of VE-cadherin (16,18) and the downregulation of ZO-1 expression (16).

Pharmacological compounds that can maintain the homeostasis of endothelial junctions have attracted attention due to their potential clinical applicability in alleviating vascular diseases (19-21). Rosmarinic acid (RA; also known as α-O-caffeoyl-3,4-dihydroxyphenyl lactic acid) is a polyphenolic antioxidant that can be found in the Lamiaceae family of herbs and mint, such as *Rosmarinus officinalis* (22). RA has been reported to exert antioxidant and anti-inflammatory activities. In particular, the antidiabetic and cardioprotective activities of RA have been previously highlighted (23,24). It was demonstrated that oxLDL-mediated oxidative stress can upregulate thioredoxin interacting protein (TXNIP) expression, which then binds to nucleotide-binding domain and leucine-rich repeat containing family, pyrin domain-containing 3 (NLRP3) to activate the NLRP3 inflammasome in ECs under HG conditions (25). RA was found

to reverse this form of oxLDL-mediated oxidative stress and NLRP3 inflammasome activation (25). In addition, the subsequent oxLDL-mediated IL-1β secretion in ECs was reversed by RA treatment by downregulating ROS production, p38 phosphorylation and forkhead box O1 (FOXO1) protein expression in ECs (25). However, the potential effect of oxLDL-triggered NLRP3 activation on endothelial integrity, permeability and monocyte transmigration remains poorly understood. In addition, the potential effect of RA on these oxLDL-mediated pathophysiological processes along with its underlying mechanism remain unknown.

Therefore, in the present study, the effects of oxLDL-triggered NLRP3 activation on the interaction between ECs and monocytes, in addition to endothelial integrity and permeability, under HG conditions, were evaluated. Specific research emphasis was placed on the possible effects of RA on these oxLDL-mediated events in the endothelium.

Materials and methods

Materials. Low-glucose DMEM (cat. no. SH30021.01), high-glucose DMEM (cat. no. SH30243.01), RPMI-1640 (cat. no. SH30027.01), fetal bovine serum (FBS; cat. no. SH30070.03), penicillin-streptomycin 100X solution (cat. no. SV30010) and 0.05% trypsin-EDTA (cat. no. SH30236.01) were purchased from HyClone; Cytiva. RA (cat. no. R4033) and human low-density lipoprotein (LDL; cat. no. 437644) were provided by MilliporeSigma. Primary antibodies against ICAM-1 (cat. no. ab109361), VCAM-1 (cat. no. ab134047), phosphorylated (p-)-VE cadherin (Y685; cat. no. ab119785), ZO-1 (cat. no. ab96587) and TXNIP (cat. no. ab188865) were purchased from Abcam. Antibodies against phosphorylated (p-)p-38 (cat. no. 9211s) and FOXO1 (cat. no. 2880s) were purchased from Cell Signaling Technology, Inc. Antibodies against p38 (cat. no. sc-535) and total VE-cadherin (cat. no. sc-6458) were obtained from Santa Cruz Biotechnology, Inc. TurboFect transfection reagent (cat. no. R0531) was purchased from Thermo Fisher Scientific, Inc. Clarity Western Enhanced chemiluminescence western blotting detection reagent (cat. no. BR170-5061) was obtained from Bio-Rad Laboratories, Inc. BCECF (cat. no. C3411) was obtained from Sigma-Aldrich; Merck KGaA. SB203580 (cat. no. 1202) was obtained from Tocris Bioscience. AS1842856 (cat. no. 16761) was procured from Cayman Chemical Company. All other reagents, including MitoTEMPO (cat. no. SML0737), Ac-YVAD-cmk (cat. no. SML0429), 2-mercaptoethanol, protease inhibitor cocktail (cat. no. P8340), 2',7'-dichlorodihydrofluores-cein diacetate (cat. no. D6883), N-acetyl-L-cysteine (NAC; cat. no. A9165), SB203580 (cat. no. S8307) and the β-actin antibody (cat. no. a2066), were all obtained from Sigma-Aldrich; Merck KGaA.

Preparation of oxLDL. oxLDL was prepared as described previously by Jin *et al* (26). Briefly, human LDL (2 mg/363 μl of 150 mM NaCl, pH 7.5, 0.01% EDTA) was added with 1xPBS to make final concentration of 2 mg/1 ml. Then, human LDL was dialyzed against PBS for 16 h at 4°C to remove EDTA and then oxidized with 5 μM $CuSO_4$ for 16 h at 37°C. The extent of LDL oxidation was assessed by measuring the formation of thiobarbituric acid-reactive substances (TBARS; cat. no. 10009055;

Cayman Chemical Company) at a wavelength of 540 nm using a microplate reader (VersaMax Microplate Reader; Molecular Devices, LLC). The level of TBARS for oxLDL and native LDL was 13.5±0.5 and 2.5±0.4, respectively.

Cell culture and treatment. The human umbilical vein endothelial cell line EA.hy926 (cat. no. ATCC-CRL-2922) and human monocyte cell line THP-1 were originally obtained from the American Type Culture Collection. EA.hy926 cells and THP-1 cells were grown in DMEM and RPMI-1640 medium, both supplemented with 10% FBS, 100 IU/ml penicillin and 10 μg/ml streptomycin, respectively. All cells were maintained in a humidified incubator at 37˚C with 5% CO_2. ECs were cultured under HG conditions (25 mM) for 48 h at 37˚C and pre-treated with Ac-YVAD-cmk (20 μM), NAC (3 mM), mito-TEMPO (20 μM), AS1842856 (50 nM), SB203580 (0.5 μM) or RA (1, 10, 50 and 100 μM) prior to oxLDL treatment for 1 h at 37˚C. Subsequently, 50 μl oxLDL stock solution (2 mg/ml) per 1 ml media was added for additional 24 h at 37˚C.

Gene silencing with siRNA. Cells were transfected with 100 nM TXNIP-targeting small interfering RNA (siTXNIP; sense, 5'-GCCGUUAGGAUCCUGGCUUTT-3' and antisense, 5'-AAGCCAGGAUCCUCCUAACGGCTT-3'; Bioneer Corporation) or control small interfering RNA (siCTRL; sense, 5'-CCUACGCCACCAAUUUCGU-3' and antisense, 5'-ACGAAAUUGGUGGCGUAGG-3'; Bioneer Corporation) by using the Turbofect transfection reagent (cat. no. R0531; Thermo Fisher Scientific, Inc.) according to the manufacturer's protocols. Briefly, ECs were transfected with control siRNA (100 nM) or TNXIP siRNA (100 nM) in the HG conditions (25 mM) for 48 h and changed with fresh medium before being stimulated with oxLDL (100 μg/ml) for an additional 12 h. After incubation for total 60 h at 37˚C, gene silencing efficiency was determined by western blot analysis.

Adhesion assay. EA.hy926 cells ($4x10^5$ cells/ml) were seeded in six-well plates and cultured until ~90% confluence under HG conditions (25 mM) for 48 h at 37˚C before being treated with oxLDL in the presence or absence of caspase-1, ROS, p38 MAPK and TXNIP inhibitors or RA at the indicated concentrations (1, 10, 50 and 100 μM) for an additional 24 h at 37˚C. THP-1 cells ($7x10^5$ cells per well) were labeled with the BCECF fluorescent dye for 30 min at 37˚C, before being added onto the ECs and incubated for 30 min at 37˚C. Following incubation, non-adherent cells were washed three times with PBS and the number of THP-1 cells adhered onto the EC cells was counted using a fluorescence microscope (Eclipse Ti-U, Nikon Corporation). Images were acquired at x200 magnification from five randomly selected fields per well. Adhered cells were counted using ImageJ version 5.2.0 software (National Institutes of Health).

Transmigration assay. To study the transmigration of THP-1 cells through an EC monolayer, a Transwell system (Falcon® Permeable Support for 24-well Plate with 8.0-μm Transparent PET Membrane; Corning, Inc.) was used. ECs ($1x10^5$ cells) cultured in DMEM supplemented with 10% FBS, 100 IU/ml penicillin and 10 μg/ml streptomycin were first seeded into the upper chambers of the Transwell chamber and placed into a

24-well plate. After 4 h at 37˚C, THP-1 cells ($5x10^5$ cells) were then added to the upper chambers of the Transwell chamber before RPMI medium supplemented with 10% FBS was added into the lower chambers. The migration chambers were then incubated for 24 h in a 37˚C cell culture incubator. The number of cells that migrated across the EC monolayer into the lower chamber was immediately counted using 0.4% tryptophan blue staining at room temperature and a Countess II automated cell counter (Thermo Fisher Scientific, Inc.).

Proteins extraction and western blotting. ECs were lysed in RIPA buffer (25 mM Tris-HCl, pH 7.4, 150 mM NaCl, 1% NP-40, 1% sodium deoxycholate and 0.1% SDS) containing a protease inhibitor cocktail. The supernatant was collected after centrifugation at 12,000 x g for 20 min at 4˚C and the protein concentration was quantified by using Bradford assay. Aliquots of 20-60 μg total protein from the different experimental groups were then analyzed. The cell homogenates were denatured with 4X SDS sample buffer containing 5% 2-mercaptoethanol, boiled for 5 min at 95˚C, loaded into a 8-10% SDS-polyacrylamide gel and separated by electrophoresis for 200 min at 100 V. The protein samples were then transferred onto PVDF membranes for 90 min at 190 mA using a wet transfer system (Bio-Rad Laboratories, Inc.). The membranes were blocked with 5% fat-free dried milk in 1X Tris buffered saline-containing 0.05% Tween-20 (TBS-T) for 1 h at room temperature and then probed with ICAM-1 (1:1,000), VCAM-1 (1:1,000), p-VE-cadherin (1:1,000), VE-cadherin (1:2,000), ZO-1 (1:1,000), p-p38 (1:1,000), p38 (1:2,000), FOXO-1 (1:500), TXNIP (1:1,000) or β-actin (1:5,000) primary antibodies overnight at 4˚C. Following primary antibody incubation, the membranes were washed with 1X TBS-T and incubated with HRP-conjugated anti-rabbit, anti-mouse or anti-goat secondary antibodies (1:5,000) for 1 h at room temperature. The immunoreactive bands were visualized by Clarity Western ECL reagent according to the manufacturer's protocol. The relative level of each protein was normalized to the level of β-actin as a loading control. Protein densities were quantified using ChemiDOC™ XRS+ Systems with Image Lab™ Software Version 5.2 (Bio-Rad Laboratories, Inc.).

Statistical analysis. The data were analyzed using GraphPad Prism 7 software (GraphPad Software, Inc.). One-way analyses of variance followed by Tukey's multiple-range test or two-way analyses of variance followed by Bonferroni's test were used to detect significant differences among the mean values. Data are presented as the means ± standard from ≥ three independent experimental repeats. $P<0.05$ was considered to indicate a statistically significant difference.

Results

oxLDL-mediated expression of ICAM-1 and VCAM-1 in ECs under HG conditions is ROS-, p38-, FOXO1/TXNIP-dependent but RA reduces oxLDL-mediated ICAM-1 and VCAM-1 expression. In a previous study (25), RA reversed oxLDL-mediated NLRP3 inflammasome activation by down-regulating ROS production, p38 phosphorylation and FOXO1 protein expression in ECs. Therefore, in the present study, the

effects of oxLDL-mediated NLRP3 activation on the expression of adhesion molecules ICAM-1 and VCAM-1 under HG conditions were first examined. Afterwards, the effects of RA on oxLDL-mediated ICAM-1 and VCAM-1 expression were examined. After the ECs were stimulated with oxLDL (100 μg/ml) under low glucose or HG conditions, the expression of ICAM-1 and VCAM-1 were found to be significantly increased, though the magnitude of increase was markedly greater following stimulation under HG conditions (Fig. S1). However, HG conditions without oxLDL stimulation did not result in any changes in the expression of ICAM-1 and VCAM-1 (Fig. S1). oxLDL-mediated ICAM-1 and VCAM-1 expression under HG conditions were found to be significantly reversed by the selective and irreversible inhibitor of caspase-1 Ac-YVAD-cmk (Fig. 1A). Next, the effects of ROS production on oxLDL-mediated ICAM-1 and VCAM-1 expression in ECs under HG conditions were investigated. ROS scavengers mitoTEMPO and NAC were found to significantly reverse oxLDL-induced ICAM-1 and VCAM-1 upregulation in the ECs under HG conditions (Fig. 1B). In addition, the p38 and FOXO1 pathway was potently activated in ECs treated with oxLDL under HG conditions, compared to low glucose conditions (Fig. S2). Therefore, the effects p38 and FOXO1 pathway activation on the upregulation of ICAM-1 and VCAM-1 in ECs stimulated with oxLDL under HG conditions were next tested. The results showed that the p38 inhibitor SB203580 and the FOXO1 inhibitor AS1842856 significantly reversed the oxLDL-induced expression of ICAM-1 and VCAM-1 in ECs under HG conditions (Fig. 1C). Subsequently, transfection with siTXNIP, which significantly knocked down TXNIP expression induced by oxLDL under HG conditions (Fig. S3), also significantly reversed the oxLDL-induced expression of ICAM-1 and VCAM-1 in ECs under HG conditions (Fig. 1D). Finally, oxLDL-mediated ICAM-1 and VCAM-1 upregulation in ECs under HG conditions was found to be significantly reduced by RA in a dose-dependent manner (Fig. 1E). Therefore, the RA-mediated decrease in ICAM-1 and VCAM-1 expression in ECs was possibly dependent on the inhibition of ROS production, p38 phosphorylation, FOXO1 and TXNIP induction.

RA reverses oxLDL-induced endothelial junction permeability under HG conditions. Next, to determine if oxLDL-induced inflammasome activation can increase EC permeability under HG conditions, VE-cadherin phosphorylation and ZO-1 expression were measured in ECs following stimulation with oxLDL under HG conditions. Consistent with the ICAM-1 and VCAM-1 expression results, oxLDL stimulation under HG conditions significantly increased the phosphorylation of VE-cadherin and decreased the expression of ZO-1 in ECs, which was in turn significantly reversed by pretreatment with Ac-YVAD-cmk (Fig. 2A), ROS scavengers mitoTEMPO and NAC (Fig. 2B) or p38 and FOXO1 inhibitors SB203580 and AS1842856, respectively (Fig. 2C). TXNIP knockdown also significantly decreased VE-cadherin phosphorylation whilst restoring ZO-1 downregulation in the presence of oxLDL under HG conditions (Fig. 2D). Furthermore, RA was found to reverse EC dysfunction caused by oxLDL treatment under HG conditions by restoring endothelial junction integrity under HG

conditions. As shown in Fig. 2E, RA significantly reversed the oxLDL-induced increases in p-VE-cadherin levels under HG conditions and oxLDL-induced decreases in ZO-1 expression under HG conditions at 50 and 100 μM.

Inhibitory effects of RA on HG- and oxLDL-induced THP-1 monocyte adhesion to ECs is dependent on the ROS-TXNIP/NLRP3 signaling pathway. Next, the effects of inhibiting the expression of adhesion molecules in ECs on THP-1 adhesion to ECs were next investigated. Consistent with the expression data of adhesion molecules aforementioned, Ac-YVAD-cmk (Fig. 3A), the ROS scavengers MitoTEMPO and NAC (Fig. 3B) and both p38 and FOXO1 inhibitors (Fig. 3C) significantly reversed the oxLDL-induced adhesion of THP-1 monocytes to ECs under HG conditions. In addition, Fig. 3D revealed that TXNIP knockdown significantly reversed oxLDL-triggered THP-1 cells adhesion to ECs under HG conditions. RA was also found to significantly diminish oxLDL-induced THP-1 monocyte adhesion to ECs under HG conditions (Fig. 3E). These findings suggest that RA effectively inhibits oxLDL-mediated THP-1 adhesion to ECs under HG conditions through downregulation of adhesion molecule (ICAM-1 and VCAM-1) expression.

oxLDL increases THP-1 monocyte diapedesis under HG conditions in a manner that can be reversed by RA. Subsequently, the effects of oxLDL on THP-1 transmigration through the EC monolayer under HG conditions and the effects of RA on THP-1 transmigration through ECs induced by oxLDL and HG were all examined (Fig. 4A). oxLDL-treated ECs under HG conditions resulted in significantly higher THP-1 transmigration levels through ECs compared with those in untreated control cells, which were in turn significantly reversed by Ac-YVAD-cmk (a caspase-1 inhibitor), MitoTEMPO and NAC (ROS scavengers), SB203580 (a p38 MAPK inhibitor) and AS1842856 (a FOXO1 inhibitor) treatment (Fig. 4B). THP-1 transmigration was significantly reduced on TXNIP siRNA-transfected ECs treated with oxLDL under HG conditions compared with that on CTRL siRNA-transfected ECs (Fig. 4C). RA also significantly reversed oxLDL-induced monocyte transmigration through ECs under HG conditions at 50 and 100 μM (Fig. 4D). These findings suggest that RA can alleviate oxLDL-induced endothelial hyperpermeability and consequent THP-1 transmigration under HG conditions.

Discussion

Endothelial dysfunction is considered to be one of the first stages of atherosclerosis under hyperglycemic and dyslipidemic conditions (27). Endothelial dysfunction increases the expression of adhesion molecules ICAM-1 and VCAM-1 by ECs, which increases the adhesion of monocytes to ECs to facilitate their diapedesis into the subendothelial space, which activates atherosclerotic plaque generation (11). Various pathological conditions, including diabetes and obesity, perturb the integrity of cell junctions, resulting in the increased movement of monocytes and plasma lipoproteins into the intima (20,28). Therefore, regulating the interaction between monocytes and ECs, in addition to endothelial permeability, would greatly limit the instigation of atherogenesis. The overexpression of
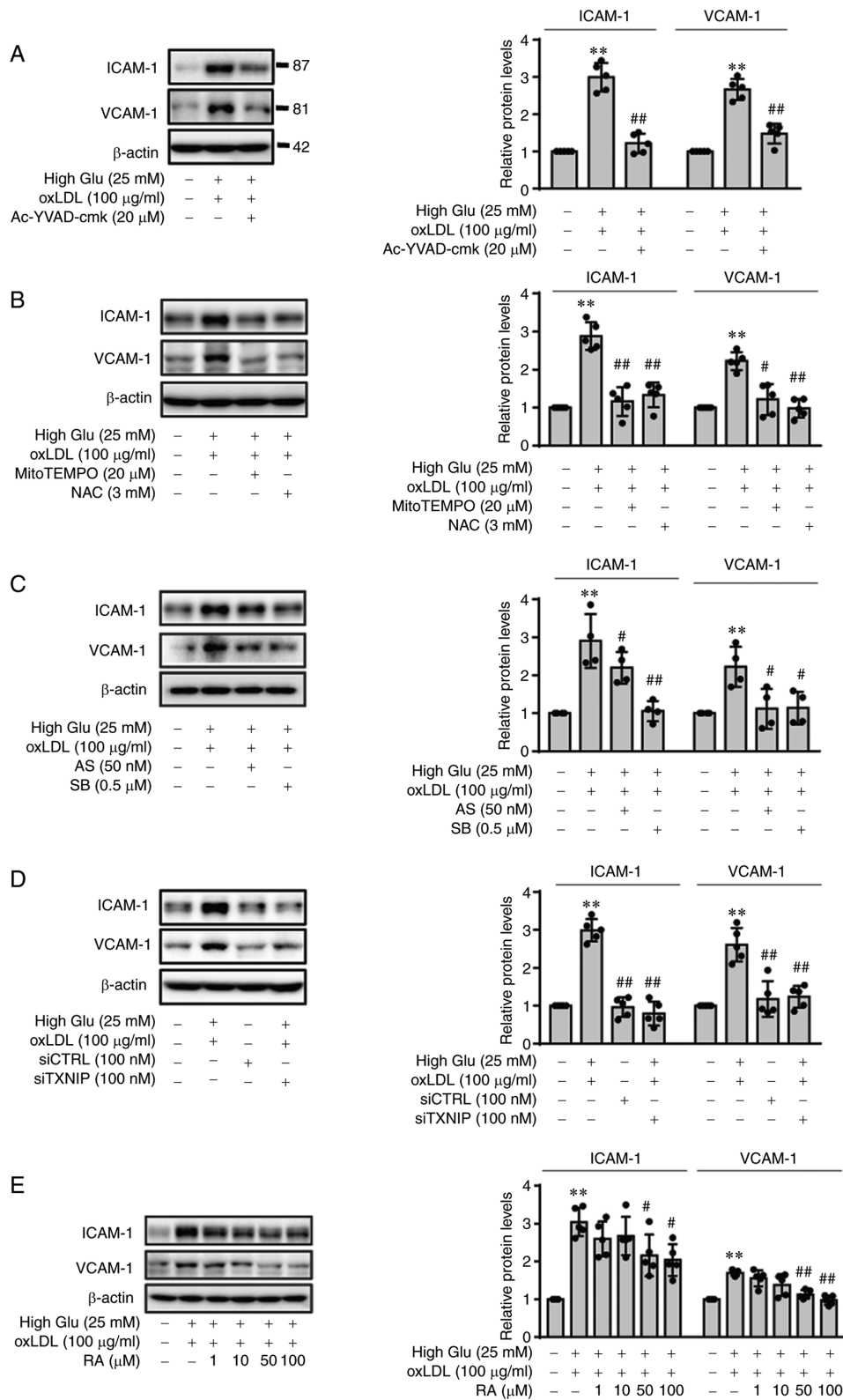
Figure 1. RA inhibits oxLDL-mediated ICAM-1 and VCAM-1 expression in ECs n under HG conditions by downregulating inflammasome activation in a ROS production, p38 MAPK and FOXO1/TXNIP-dependent manner. ECs were cultured under HG conditions (25 mM) for 48 h and pre-treated with (A) an irreversible inhibitor of IL-1β Ac-YVAD-cmk (20 μM), (B) the ROS inhibitor NAC (3 mM) or the mitochondrial ROS inhibitor mitoTEMPO (20 μM) or (C) the FOXO1 inhibitor AS1842856 (50 nM) or the p38 MAPK inhibitor SB203580 (0.5 μM), prior to oxLDL treatment. The ECs were then lysed 24 h later before ICAM-1 and VCAM-1 protein expression were measured by western blotting. (D) CTRL siRNA- or TXNIP siRNA-transfected ECs were cultured under HG conditions (25 mM) for 48 h before being stimulated with oxLDL for 24 h. ICAM-1 and VCAM-1 protein expression were measured in the lysates by western blotting. (E) ECs were cultured under HG conditions (25 mM) for 48 h and stimulated with oxLDL for 24 h in the presence of RA (0, 1, 10, 50 and 100 mM), before ICAM-1 and VCAM-1 protein expression were measured by western blotting. Band densities were quantified and relative protein expression are presented as the mean ± SD from five independent experiments. **P<0.01 vs. untreated control. $^{#}$P<0.05 and $^{##}$P<0.01 vs. HG + oxLDL. RA, Rosmarinic acid; ICAM-1, intercellular adhesion molecule-1; VCAM-1, vascular cell adhesion molecule-1; ECs, endothelial cells; High Glu or HG, high glucose; ROS, reactive oxygen species; FOXO1, forkhead box O1; TXNIP1, thioredoxin interacting protein; NAC, N-acetyl-L-cysteine; oxLDL, oxidized low density lipo-protein; AS, AS1842856; SB, SB203580; si, small-interfering; CTRL, control.
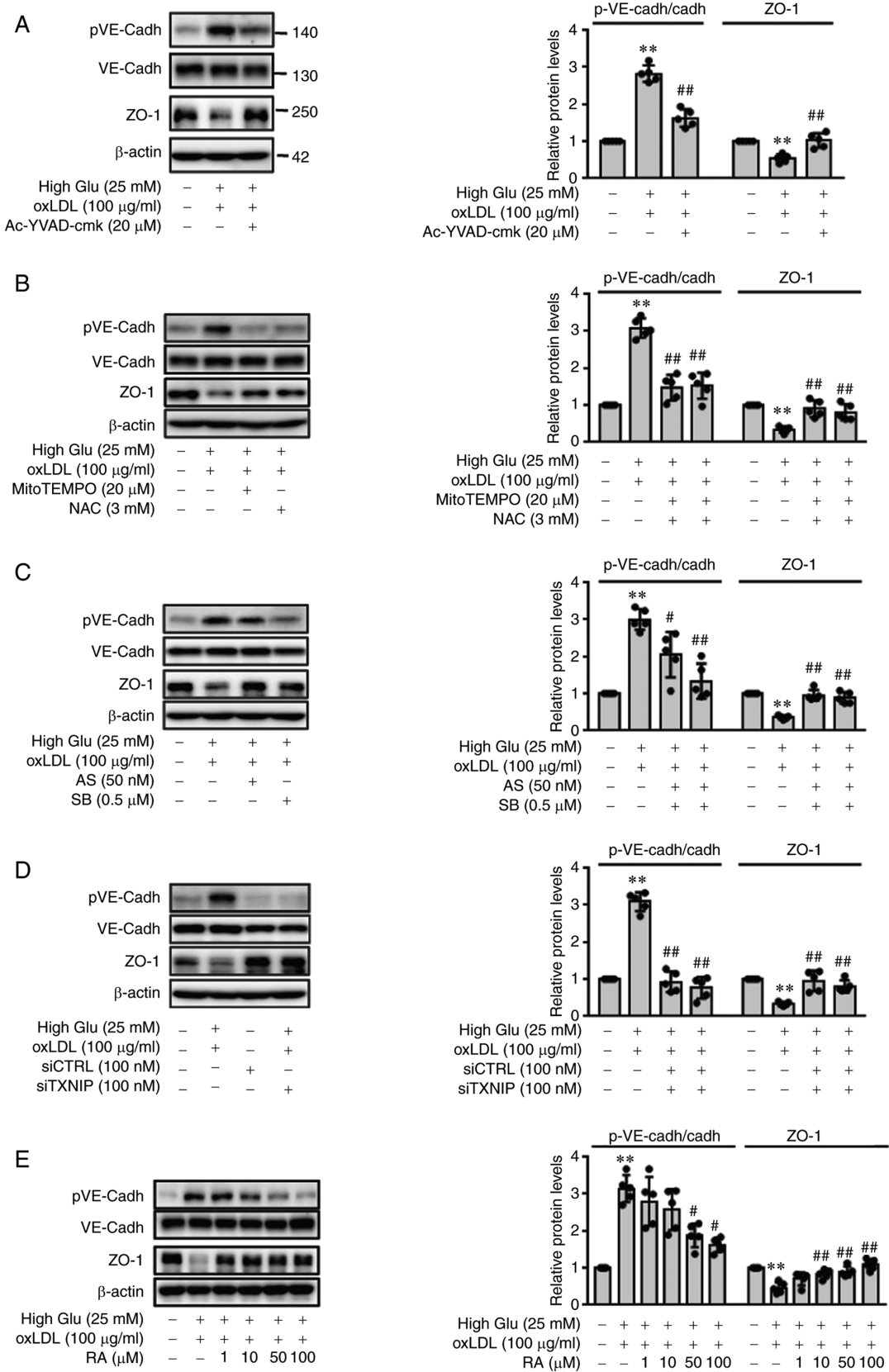
Figure 2. oxLDL promotes endothelial permeability under HG conditions by phosphorylating VE-cadherin and reducing the expression of ZO-1 in a RA-dependent manner. (A-E) pVE-cadherin and ZO-1 protein levels in the cell lysates were measured by western blot analysis. ECs cultured under HG conditions were pre-treated with (A) Ac-YVAD-cmk (20 μM), (B) NAC (3 mM) or mitoTEMPO (20 μM) or (C) AS1842856 (50 nM) or SB203580 (0.5 μM) for 1 h, before being stimulated with oxLDL for 24 h. (D) CTRL siRNA- or TXNIP siRNA-transfected ECs were cultured under HG conditions (25 mM) for 48 h and stimulated with oxLDL for 24 h. (E) ECs were cultured under HG conditions (25 mM) for 48 h and then stimulated with oxLDL for an additional 24 h in the presence or absence of RA (0, 1, 10, 50 and 100 μM). Band densities were quantified and relative protein levels are presented as the mean ± SD from five independent experiments. **$P<0.01$ vs. Control; #$P<0.05$ and ##$P<0.01$ vs. HG + oxLDL group. RA, Rosmarinic acid; p, phosphorylated; VE-cadh, vascular endothelial cadherin; ZO-1, zonula occludens; ECs, endothelial cells; High Glu or HG, high glucose; TXNIP1, thioredoxin interacting protein; NAC, N-acetyl-L-cysteine; oxLDL, oxidized low density lipoprotein; AS, AS1842856; SB, SB203580; si, small-interfering; CTRL, control.
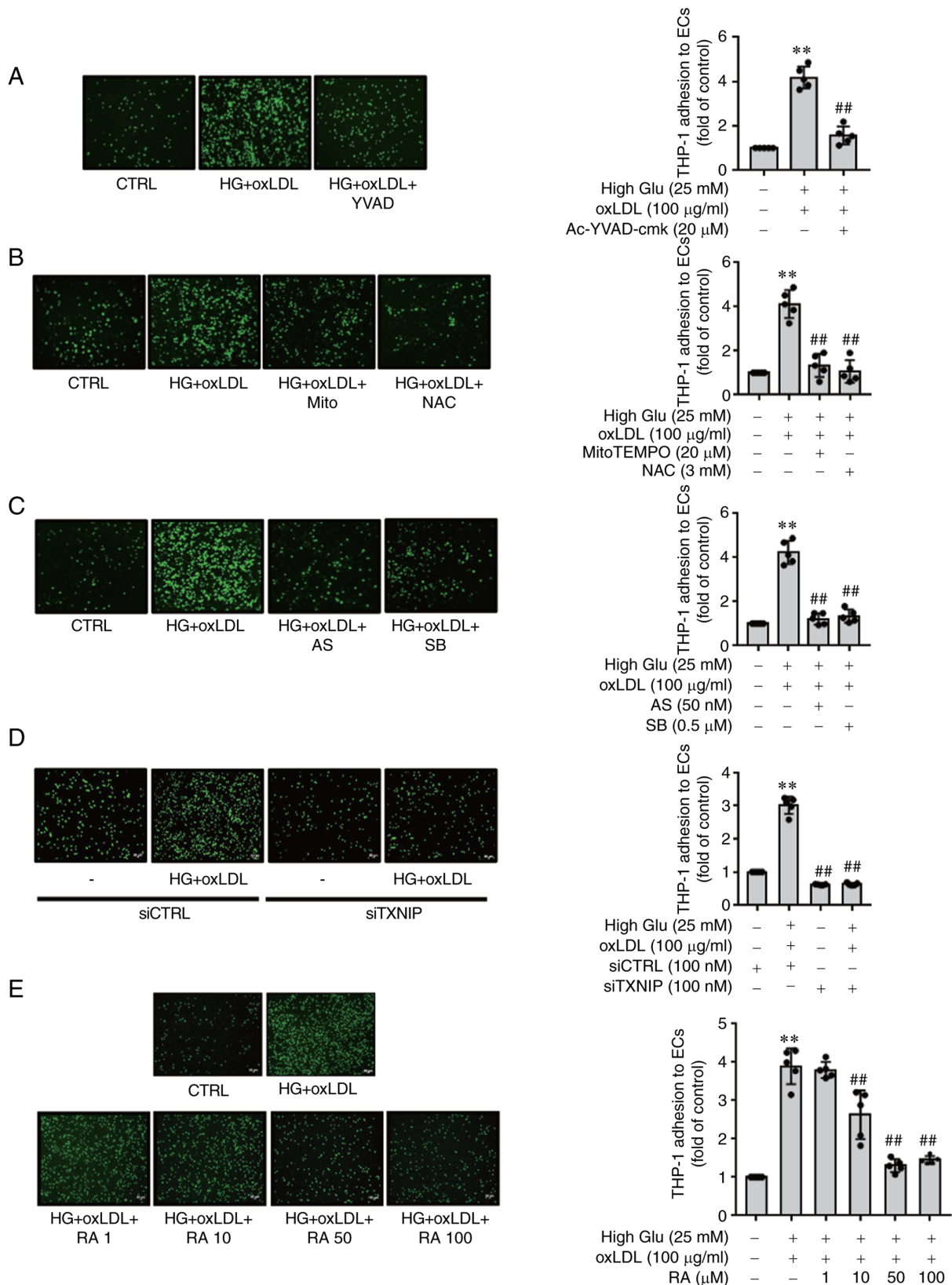
Figure 3. RA reduces the oxLDL-induced adherence of THP-1 monocytes onto the endothelial monolayer under HG conditions by downregulating reactive oxygen species production, p38 MAPK activation and forkhead box O1/thioredoxin interacting protein-induced inflammasome activation. (A-E) THP-1 cells ($7x10^5$ cells/ml) were added to the ECs. After 30 min at 37˚C, cell suspensions were withdrawn and the ECs were gently washed three times with PBS. The adherent cells were then counted under a fluorescence microscope. ECs cultured under HG conditions were pretreated with (A) Ac-YVAD-cmk (20 μM), (B) NAC (3 mM) or mitoTEMPO (20 μM) or (C) AS1842856 (50 nM) or SB203580 (0.5 μM) for 1 h before being stimulated with oxLDL for 24 h. (D) CTRL siRNA- or TXNIP siRNA-transfected ECs were cultured under HG conditions (25 mM) for 48 h and stimulated with oxLDL for 24 h. (E) ECs were cultured under HG conditions (25 mM) for 48 h and stimulated with oxLDL for an additional 24 h in the presence of RA (0, 1, 10, 50 and 100 μM). Values are expressed as the mean ± SD from five independent experiments. **P<0.01 vs. Control; $^{##}$P<0.01 vs. HG + oxLDL group. RA, Rosmarinic acid; oxLDL, oxidized low density lipoprotein; ECs, endothelial cells; High Glu or HG, high glucose; TXNIP1, thioredoxin interacting protein; NAC, N-acetyl-L-cysteine; AS, AS1842856; SB, SB203580; si, small-interfering; CTRL, control.
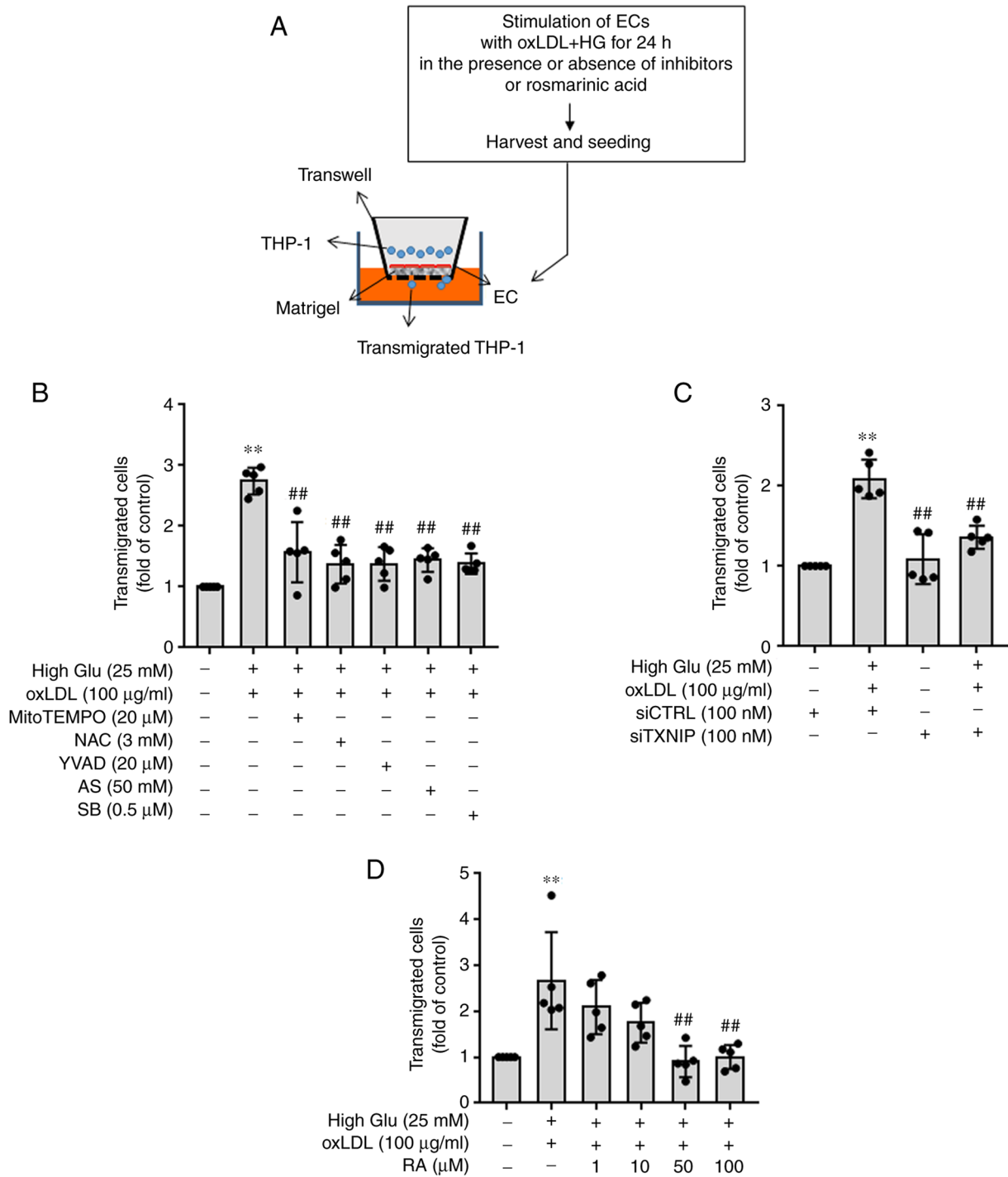
Figure 4. oxLDL and HG treatment promotes the transmigration of monocytes through ECs by modulating the inflammasome activation pathway in a manner that can be reversed by RA. (A) ECs were added to Matrigel-coated insert wells. ECs cultured under HG conditions (25 mM) for 48 h were stimulated with oxLDL in the presence of inhibitors or RA for 24 h before being harvested and added to Matrigel-coated insert wells. THP-1 cells were then added to ECs 4 h later. The migration chambers were incubated for 24 h. The number of cells that migrated across the EC monolayer into the lower chamber was counted using tryptophan blue staining and a Countess II automated cell counter. (B) ECs cultured under HG conditions (25 mM) were pretreated with mitoTEMPO (20 μM), NAC (3 mM), Ac-YVAD-cmk (20 μM), AS1842856 (50 nM) or SB203580 (0.5 μM) for 1 h before being stimulated with oxLDL for an additional 24 h. (C) CTRL siRNA- or TXNIP siRNA-transfected ECs were cultured under HG conditions (25 mM) and stimulated with oxLDL. (D) ECs cultured under HG conditions (25 mM) were stimulated with oxLDL for an additional 24 h in the presence or absence of RA (0, 1, 10, 50 and 100 μM). Values are expressed as the mean ± SD from five independent experiments. **P<0.01 vs. Control; ##P<0.01 vs. HG + oxLDL. RA, Rosmarinic acid; oxLDL, oxidized low density lipoprotein; ECs, endothelial cells; High Glu or HG, high glucose; TXNIP1, thioredoxin interacting protein; NAC, N-acetyl-L-cysteine; AS, AS1842856; SB, SB203580; si, small-interfering; CTRL, control.

endothelial adhesion molecules has been previously reported to be key for the pathogenesis of vascular diseases, such as atherosclerosis (29,30). In addition, HG conditions and oxLDL further contribute to the development of atherosclerosis by increasing the expression of ICAM-1 and VCAM-1 (31,32). Previous studies have documented that inflammatory

cytokines, such as TNF-α, IL-33 and IL-1β, was positively associated with the increased expression of VCAM-1 and ICAM-1 in vascular and cardiac cells, leukocyte adhesion to ECs and endothelial hyperpermeability (33-35).

RA has been previously reported to exert beneficial effects on the cardiovascular system because of its antioxidant and anti-inflammatory properties. It reduced adriamycin-induced cardiotoxicity in H9C2 cells by inhibiting ROS production (36), in addition to inhibiting atherosclerotic plaque formation in Apolipoprotein E$^{-/-}$ mice fed on a high-cholesterol diet, by reducing the serum levels of proinflammatory cytokines TNF-α and IL-1β (37). In a previous study, it was shown that RA protected ECs by inhibiting oxLDL-mediated NLRP3 inflammasome activation and resultant IL-1β production under HG conditions (25). Therefore, for further study, the present study investigated the effects of RA on oxLDL-mediated interactions between monocytes and ECs, endothelial permeability and transmigration of monocytes through endothelial monolayers. ECs stimulated with oxLDL under HG conditions were found to exhibit significantly higher expression levels of adhesion molecules ICAM-1 and VCAM-1, which resulted in increased THP-1 monocyte adhesion onto EC monolayer. oxLDL-induced endothelial inflammation under HG conditions has been reported to be orchestrated by ROS-mediated p38 phosphorylation, FOXO1/TXNIP induction and IL-1β production (25,38,39). Correspondingly, ECs pretreated with the irreversible inhibitor of caspase-1 (an IL-1β converting enzyme), ROS scavengers and p38 and FOXO1 inhibitors all showed significant reductions in oxLDL-induced ICAM-1 and VCAM-1 protein expression under HG conditions. Notably, TXNIP knockdown also reversed HG- and oxLDL-mediated overexpression of ICAM-1 and VCAM-1 in ECs. In particular, inhibitors of ROS, p38 MAPK, FOXO1 and TXNIP, all of which are involved in the expression of the adhesion molecules ICAM-1 and VCAM-1, significantly reduced oxLDL-induced THP-1 monocyte adhesion to ECs under HG conditions. RA, which was previously found to downregulate the activity of the p38/FOXO1/TXNIP pathway and inhibit inflammasome activation in oxLDL- and HG-stimulated ECs (22), diminished oxLDL-mediated upregulation of ICAM-1 and VCAM-1 expression in ECs under HG conditions whilst significantly reducing THP-1 monocyte adhesion to ECs in a dose-dependent manner. oxLDL-induced expression of adhesion molecules (ICAM-1 and VCAM-1) was found to be markedly higher under HG conditions compared with that stimulated under low glucose conditions. In addition, oxLDL treatment increased the levels of NLRP3 activation pathway mediators p-p38, FOXO-1 and TXNIP under low glucose conditions, which were enhanced under HG conditions. However, HG without oxLDL stimulation did not exert any changes in the expression of ICAM-1 and VCAM-1 whilst weakly increasing p-p38, FOXO-1 and TXNIP levels. These results suggest that oxLDL enhances the inflammatory response under HG conditions but not under low glucose conditions or HG conditions without oxLDL.

Endothelial inflammation alters junction integrity and increases endothelial permeability (40,41). Vascular permeability and monocyte diapedesis are increased by the phosphorylation of VE-cadherin, a major component of adherens junctions (18,42), and by the downregulation of ZO-1, a key molecule of tight junctions (16). HG and oxLDL were
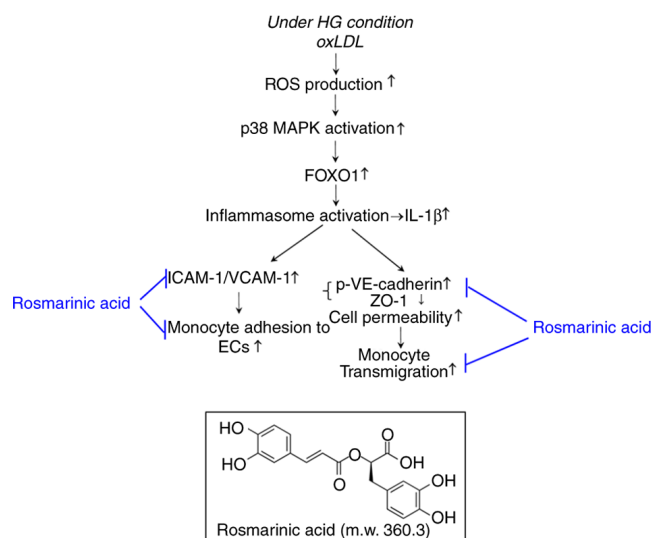

Figure 5. Schematic model of the underlying mechanism of the rosmarinic acid-mediated reversal of oxLDL-mediated endothelial dysfunction under HG conditions by modulating the interaction between monocytes and ECs. oxLDL, oxidized low density lipoprotein; HG, high glucose; ROS, reactive oxygen species; FOXO1, forkhead box O1; ICAM1, intercellular adhesion molecule-1; VCAM-1, vascular cell adhesion molecule-1; ECs, endothelial cells; p-, phosphorylated; VE, vascular endothelial; ZO-1, zonula occludens-1; m.w., molecular weight.

found to increase VE-cadherin phosphorylation but decrease ZO-1 expression in ECs in the present study, which in turn significantly induced THP1 monocyte transmigration through ECs. Pretreatment of the ECs with ROS scavengers, inhibitors of caspase-1, p38 MAPK and FOXO1 and transfection with TXNIP siRNA all reversed the oxLDL-induced phosphorylation of VE-cadherin and ZO-1 downregulation under HG conditions. In addition, inhibiting ROS/p38 MAPK/TXNIP inflammasome pathway activation significantly reduced monocyte diapedesis through the EC monolayers. RA also reversed the oxLDL-increased phosphorylation of VE-cadherin and downregulation of ZO-1 expression in a dose-dependent manner, which resulted in the blockage of monocyte diapedesis through EC monolayers.

Taken together, results of the present study revealed that oxLDL can trigger the overexpression of adhesion molecules in ECs under HG conditions, which leads to the adhesion of monocytes to ECs. In addition, oxLDL stimulation increases endothelial permeability, promoting monocyte diapedesis. Based on previous findings and the results of this study, RA effectively prevented the expression of adhesion molecules and THP-1 monocyte adhesion to ECs whilst inhibiting endothelial monolayer leakage and THP-1 monocyte diapedesis, by regulating oxLDL-mediated ROS/p38 MAPK/FOXO1/TXNIP/inflammasome activation under HG conditions (Fig. 5). These findings suggest that RA exerts protective effects against hyperlipidemia- and hyperglycemia-induced cardiovascular disease by modulating the interaction between monocytes and ECs, as well as monocyte diapedesis.

Acknowledgements

Funding

Availability of data and materials

The datasets used and/or analyzed during the current study are available from the corresponding author on reasonable request.

Authors' contributions

JBN performed the experiments and analyzed the data. YSK and HJ performed the experiments and analyzed the data. SWP and SPY contributed to the analysis and the interpretation of the data. KRK provided important critical feedback on data interpretation and revision. HJK designed the study, interpreted the data and revised the manuscript. JBN, YSK and HJK confirmed the authenticity of all the raw data. All authors read and approved the final manuscript.

Ethics approval and consent to participate

Not applicable.

Patient consent for publication

Not applicable.

Competing interests

The authors declare that they have no competing interests.

References

1. Sluiter TJ, van Buul JD, Huveneers S, Quax PHA and de Vries MR: Endothelial barrier function and leukocyte transmigration in atherosclerosis. Biomedicines 9: 328, 2021.
2. Taddei A, Giampietro C, Conti A, Orsenigo F, Breviario F, Pirazzoli V, Potente M, Daly C, Dimmeler S and Dejana E: Endothelial adherens junctions control tight junctions by VE-cadherin-mediated upregulation of claudin-5. Nat Cell Biol 10: 923-934, 2008.
3. Chistiakov DA, Orekhov AN and Bobryshev YV: Endothelial barrier and its abnormalities in cardiovascular disease. Front Physiol 6: 365, 2015.
4. Sena CM, Pereira AM and Seiça R: Endothelial dysfunction-a major mediator of diabetic vascular disease. Biochim Biophys Acta 1832: 2216-2231, 2013.
5. Bai B, Yang Y, Wang Q, Li M, Tian C, Liu Y, Aung LH, Li PF, Yu T and Chu XM: NLRP3 inflammasome in endothelial dysfunction. Cell Death Dis 11: 776, 2020.
6. Katakami N: Mechanism of development of atherosclerosis and cardiovascular disease in diabetes mellitus. J Atheroscler Thromb 25: 27-39, 2018.
7. Mittal M, Siddiqui MR, Tran K, Reddy SP and Malik AB: Reactive oxygen species in inflammation and tissue injury. Antioxid Redox Signal 20: 1126-1167, 2014.
8. Hamed S, Brenner B, Abassi Z, Aharon A, Daoud D and Roguin A: Hyperglycemia and oxidized-LDL exert a deleterious effect on endothelial progenitor cell migration in type 2 diabetes mellitus. Thromb Res 126: 166-174, 2010.
9. Ko YS, Jin H, Park SW and Kim HJ: Salvianolic acid B protects against oxLDL-induced endothelial dysfunction under high-glucose conditions by downregulating ROCK1-mediated mitophagy and apoptosis. Biochem Pharmacol 174: 113815, 2020.
10. Akhmedov A, Rozenberg I, Paneni F, Camici GG, Shi Y, Doerries C, Sledzinska A, Mocharla P, Breitenstein A, Lohmann C, *et al*: Endothelial overexpression of LOX-1 increases plaque formation and promotes atherosclerosis in vivo. Eur Heart J 35: 2839-2848, 2014.
11. Matheus AS, Tannus LR, Cobas RA, Palma CC, Negrato CA and Gomes MB: Impact of diabetes on cardiovascular disease: An update. Int J Hypertens 2013: 653789, 2013.
12. Claesson-Welsh L, Dejana E and McDonald DM: Permeability of the endothelial barrier: Identifying and reconciling controversies. Trends Mol Med 27: 314-331, 2021.
13. Dejana E, Tournier-Lasserve E and Weinstein BM: The control of vascular integrity by endothelial cell junctions: Molecular basis and pathological implications. Dev Cell 16: 209-221, 2009.
14. Giannotta M, Trani M and Dejana E: VE-cadherin and endothelial adherens junctions: Active guardians of vascular integrity. Dev Cell 26: 441-454, 2013.
15. Chattopadhyay R, Dyukova E, Singh NK, Ohba M, Mobley JA and Rao GN: Vascular endothelial tight junctions and barrier function are disrupted by 15(S)-hydroxyeicosatetraenoic acid partly via protein kinase C ε-mediated zona occludens-1 phosphorylation at threonine 770/772. J Biol Chem 289: 3148-3163, 2014.
16. Tornavaca O, Chia M, Dufton N, Almagro LO, Conway DE, Randi AM, Schwartz MA, Matter K and Balda MS: ZO-1 controls endothelial adherens junctions, cell-cell tension, angiogenesis, and barrier formation. J Cell Biol 208: 821-838, 2015.
17. Orsenigo F, Giampietro C, Ferrari A, Corada M, Galaup A, Sigismund S, Ristagno G, Maddaluno L, Koh GY, Franco D, *et al*: Phosphorylation of VE-cadherin is modulated by haemodynamic forces and contributes to the regulation of vascular permeability in vivo. Nat Commun 3: 1208, 2012.
18. Wessel F, Winderlich M, Holm M, Frye M, Rivera-Galdos R, Vockel M, Linnepe R, Ipe U, Stadtmann A, Zarbock A, *et al*: Leukocyte extravasation and vascular permeability are each controlled in vivo by different tyrosine residues of VE-cadherin. Nat Immunol 15: 223-230, 2014.
19. Hsieh SL, Wang JJ, Su KH, Kuo YL, Hsieh S and Wu CC: Suppressive effects of the gynura bicolor ether extract on endothelial permeability and leukocyte transmigration in human endothelial cells induced by TNF-α. Evid Based Complement Alternat Med 2020, 9413724, 2020.
20. Lian D, Yuan H, Yin X, Wu Y, He R, Huang Y and Chen Y: Puerarin inhibits hyperglycemia-induced inter-endothelial junction through suppressing endothelial Nlrp3 inflammasome activation via ROS-dependent oxidative pathway. Phytomedicine 55: 310-319, 2019.
21. Zhou X, Wu Y, Ye L, Wang Y, Zhang K, Wang L, Huang Y, Wang L, Xian S, Zhang Y and Chen Y: Aspirin alleviates endothelial gap junction dysfunction through inhibition of NLRP3 inflammasome activation in LPS-induced vascular injury. Acta Pharm Sin B 9: 711-723, 2019.
22. Kim GD, Park YS, Jin YH and Park CS: Production and applications of rosmarinic acid and structurally related compounds. Appl Microbiol Biotechnol 99: 2083-2092, 2015.
23. Karthik D, Viswanathan P and Anuradha CV: Administration of rosmarinic acid reduces cardiopathology and blood pressure through inhibition of p22phox NADPH oxidase in fructose-fed hypertensive rats. J Cardiovasc Pharmacol 58: 514-521, 2011.
24. Sotnikova R, Okruhlicova L, Vlkovicova J, Navarova J, Gajdacova B, Pivackova L, Fialova S and Krenek P: Rosmarinic acid administration attenuates diabetes-induced vascular dysfunction of the rat aorta. J Pharm Pharmacol 65: 713-723, 2013.
25. Nyandwi JB, Ko YS, Jin H, Yun SP, Park SW and Kim HJ: Rosmarinic acid inhibits oxLDL-induced inflammasome activation under high-glucose conditions through downregulating the p38-FOXO1-TXNIP pathway. Biochem Pharmacol 182: 114246, 2020.
26. Jin H, Ko YS, Park SW and Kim HJ: P2Y$_2$R activation by ATP induces oxLDL-mediated inflammasome activation through modulation of mitochondrial damage in human endothelial cells. Free Radic Biol Med 136: 109-117, 2019.
27. Wan Z, Fan Y, Liu X, Xue J, Han Z, Zhu C and Wang Z: NLRP3 inflammasome promotes diabetes-induced endothelial inflammation and atherosclerosis. Diabetes Metab Syndr Obes 12: 1931-1942, 2019.

28. Hashimoto K, Kataoka N, Nakamura E, Tsujioka K and Kajiya F: Oxidized LDL specifically promotes the initiation of monocyte invasion during transendothelial migration with upregulated PECAM-1 and downregulated VE-cadherin on endothelial junctions. Atherosclerosis 194: e9-e17, 2007.

29. Santos JC, Cruz MS, Bortolin RH, Oliveira KM, Araújo JN, Duarte VH, Silva AM, Santos IC, Dantas JM, Paiva MS, et al: Relationship between circulating VCAM-1, ICAM-1, E-selectin and MMP9 and the extent of coronary lesions. Clinics (Sao Paulo) 73: e203, 2018.

30. Rubio-Guerra AF, Vargas-Robles H, Serrano AM, Lozano-Nuevo JJ and Escalante-Acosta BA: Correlation between the levels of circulating adhesion molecules and atherosclerosis in type-2 diabetic normotensive patients: Circulating adhesion molecules and atherosclerosis. Cell Adh Migr 3: 369-372, 2009.

31. Huang Z, Cai X, Li S, Zhou H, Chu M, Shan P and Huang W: Berberine-attenuated monocyte adhesion to endothelial cells induced by oxidized low-density lipoprotein via inhibition of adhesion molecule expression. Mol Med Rep 7: 461-465, 2013.

32. Chen JS, Chen YH, Huang PH, Tsai HY, Chen YL, Lin SJ and Chen JW: Ginkgo biloba extract reduces high-glucose-induced endothelial adhesion by inhibiting the redox-dependent interleukin-6 pathways. Cardiovasc Diabetol 11: 49, 2012.

33. Cejkova S, Kubatova H, Thieme F, Janousek L, Fronek J, Poledne R and Lesna I: The effect of cytokines produced by human adipose tissue on monocyte adhesion to the endothelium. Cell Adh Migr 13: 293-302, 2019.

34. van Wetering S, van den Berk N, van Buul JD, Mul FP, Lommerse I, Mous R, ten Klooster JP, Zwaginga JJ and Hordijk PL: VCAM-1-mediated Rac signaling controls endothelial cell-cell contacts and leukocyte transmigration. Am J Physiol Cell Physiol 285: C343-C352, 2003.

35. Demyanets S, Konya V, Kastl SP, Kaun C, Rauscher S, Niessner A, Pentz R, Pfaffenberger S, Rychli K, Lemberger CE, et al: Interleukin-33 induces expression of adhesion molecules and inflammatory activation in human endothelial cells and in human atherosclerotic plaques. Arterioscler Thromb Vasc Biol 31: 2080-2089, 2011.

36. Kim DS, Kim HR, Woo ER, Hong ST, Chae HJ and Chae SW: Inhibitory effects of rosmarinic acid on adriamycin-induced apoptosis in H9c2 cardiac muscle cells by inhibiting reactive oxygen species and the activations of c-Jun N-terminal kinase and extracellular signal-regulated kinase. Biochem Pharmacol 70: 1066-1078, 2005.

37. Li L, Tian J and Liang X: Regression of atherosclerosis by rosmarinic acid via regulating lipid metabolism and anti-inflammatory actions. J Mol Cell Cardiol 44: P719, 2008.

38. Jian D, Wang Y, Jian L, Tang H, Rao L, Chen K, Jia Z, Zhang W, Liu Y, Chen X, et al: METTL14 aggravates endothelial inflammation and atherosclerosis by increasing FOXO1 N6-methyladeosine modifications. Theranostics 10: 8939-8956, 2020.

39. Liang B, Wang X, Zhang N, Yang H, Bai R, Liu M, Bian Y, Xiao C and Yang Z: Angiotensin-(1-7) attenuates angiotensin II-induced ICAM-1, VCAM-1, and MCP-1 expression via the MAS receptor through suppression of P38 and NF-κB pathways in HUVECs. Cell Physiol Biochem 35: 2472-2482, 2015.

40. Reglero-Real N, Colom B, Bodkin JV and Nourshargh S: Endothelial cell junctional adhesion molecules: Role and regulation of expression in inflammation. Arterioscler Thromb Vasc Biol 36: 2048-2057, 2016.

41. Sukriti S, Tauseef M, Yazbeck P and Mehta D: Mechanisms regulating endothelial permeability. Pulm Circ 4: 535-551, 2014.

42. Gavard J: Endothelial permeability and VE-cadherin: A wacky comradeship. Cell Adh Migr 7: 455-461, 2013.